ELECTRO-OPTICS vs. MAGNETO-OPTICS: POWER CONSIDERATIONS

A. R. Reisinger, et al

IBM Thomas J. Watson Research Center

Prepared for:

Office of Naval Research
Advanced Research Projects Agency

November 1974

ELECTRO-OPTICS VS. MAGNETO-OPTICS: POWER CONSIDERATIONS

FINAL TECHNICAL REPORT
(January 15, 1973 - June 30, 1974)

November, 1974

by

A. R. Reisinger
C. G. Powell
S. C. Tseng (principal investigator)

Prepared under Contract N00014-73-0256

Sponsored by

Advanced Research Projects Agency

ARPA Order No. 2327
Program Code No. 6514
Amount - $49,578.00
99,000.00
$148,578.00

by

IBM Corporation
Thomas J. Watson Research Center
P. O. Box 218
Yorktown Heights, New York 10598

if

Unclassified

Security Classification

AD/A-002276

DOCUMENT CONTROL DATA - R & D

(Security classification of title, body of abstract and indexing annotation must be entered when the overall report is classified)

1. ORIGINATING ACTIVITY (Corporate author)

IBM Thomas J. Watson Research Center
P. O. Box 218
Yorktown Heights, N. Y. 10598

2a. REPORT SECURITY CLASSIFICATION

Unclassified

2b. GROUP

3. REPORT TITLE

ELECTRO-OPTICS VS. MAGNETO-OPTICS: POWER CONSIDERATIONS

4. DESCRIPTIVE NOTES (Type of report and inclusive dates)

5. AUTHOR(S) (First name, middle initial, last name)

A. R. Reisinger
C. G. Powell
S. C. Tseng (principal investigator)

6. REPORT DATE

November, 1974

7a. TOTAL NO. OF PAGES

7b. NO. OF REFS

23

8a. CONTRACT OR GRANT NO

N00014-73C-0256

b. PROJECT NO

c.

d.

9a. ORIGINATOR'S REPORT NUMBER(S)

9b. OTHER REPORT NO(S) (Any other numbers that may be assigned this report)

10. DISTRIBUTION STATEMENT

Approved for public release, distribution unlimited

11. SUPPLEMENTARY NOTES

12. SPONSORING MILITARY ACTIVITY

Advanced Research Projects Agency
ARPA Order No. 2327

13. ABSTRACT

Conventional calculations of the power per unit bandwidth, based on the evaluation of the energy stored in the active crystal, indicate that magneto-optic modulators might be more attractive than their electro-optic counterparts. However, these calculations do not take into account the dynamical response of an assembly of spins placed in a magnetic field. Whether magnetization reversal takes place by coherent rotation or domain wall motion, the switching time decreases with increasing modulating field amplitude. This behavior is expected on a theoretical basis and is well confirmed by experiments. As a corollary, the bandwidth of a m-o device can be pushed upwards only at the cost of increasing power consumption. With presently available films, the power requirements are such that magneto-optics does not appear to be competitive with electro-optics for the construction of wideband, low power, integrated optical modulators.

DD FORM 1 NOV 65 1473

Unclassified

Security Classification

14 KEY WORDS	LINK A		LINK B		LINK C	
	ROLE	WT	ROLE	WT	ROLE	WT
Magneto-optics						
Optical Waveguides						
Modulation						
Magnetization Switching						
Bandwidth						
Power requirements						

TABLE OF CONTENTS

INTRODUCTION

The Faraday effect has been recognized for some time as a potentially suitable scheme of light modulation at infrared wavelengths[1]. Early experiments involved modulation at the resonance frequency of crystals biased in a strong DC magnetic field[2,3]. These types of devices have a very narrow bandwidth inherent to a resonance phenomenon and also produce low modulation depth.

More recently, attempts have been made to use magneto-optic thin films as base-band integrated optical modulators[4,5]. The purpose of this report is to evaluate the performance of such thin film devices, particularly with regard to the power per unit bandwidth, and determine to what extent they could compete with electro-optic modulators.

In Section I, the power per unit bandwidth for typical e-o and m-o modulators is compared. The derivation is based on the evaluation of the time-averaged energy stored in the active crystal. Under the conventional assumption that the physical mechanism responsible for modulation is fast enough for the bandwidth to be determined by the driving circuit only, we find that magneto-optics would compare favorably with electro-optics in terms of power per unit bandwidth (2.5 μW/MHz as against 175 μW/MHz, for crystals of length 1 cm and cross section area 100 μ^2).

In Section II, the dynamical characteristics of spin rotation and domain wall displacement are reviewed. The result of fundamental importance to us is that the switching time in a magneto-optic medium decreases with increasing driving field. Consequently, at a given level

of field amplitude, the dynamical response of the device may well be imposed by the material itself, rather than by the driving circuit, thereby raising the power per unit bandwidth.

In Section III, our previous experiments are briefly summarized and our recent results presented. Our data confirm the fact that the bandwidth of our devices depends very strongly on the amplitude of the switching field. The dependence of switching time on driving field in our garnet samples is found to be very similar to that observed by other workers in ferromagnetic thin films.

Our conclusions are summarized in Section IV. The dynamics of the switching process plays a vital role in the evaluation of the performance of a base-band m-o modulator. While it is always possible to approach the bandwidth of the driving circuit itself, this can be accomplished only at the cost of an increasing power consumption. From this standpoint, a fast rise-time circuit is not necessarily advantageous if it requires a large current to generate the required magnetic field. Using a meander line producing about 10 Amp/Oe and of induction 0.16 μH, the power per unit bandwidth of our devices is estimated to be 500 mW/MHz. From the data published by Tien et al[4] we infer a somewhat better figure of 85 mW/MHz.

On the basis of these figures, magneto-optics does not appear to be competitive with electro-optics for wideband, low-power, integrated optical modulators. The applications of magneto-optics seems to be limited to static high efficiency mode converters and related devices such as non-reciprocal isolators, gyrators, and optical digital to analog converters.

1. ELECTRO-OPTICS VS. MAGNETO-OPTICS: POWER CONSIDERATIONS

Speed and driving power are two parameters of utmost importance in the evaluation of the performance of an integrated optical modulator. In this section, electro-optics and magneto-optics are compared on the basis of power per unit bandwidth, for which general expressions are derived.

1.1 Electro-optics

This scheme of modulation relies on the induced birefringence caused by the application of an electric field in the appropriate direction by means of electrodes as schematically illustrated in Fig. 1-a. We start by noting that the crystal is polarized by the applied electric field, causing energy to be stored in it. This energy has the well known form:

$$W = \frac{1}{2} \int \vec{D} \cdot \vec{E}^{*} \, d\tau = \frac{1}{2} \, \varepsilon_r \, \varepsilon_o \, |E|^2 \, \tau \qquad (1)$$

where ε_r is the relative dielectric permittivity, ε_o the dielectric constant of vacuum ($\varepsilon_o = 1/36\pi \times 10^9$ farad/m), E the magnitude of the electric field and τ the volume of the crystal. For simplicity, eq. (1) ignores the fact that the dielectric properties of the crystal are tensorial rather than scalar.

Upon application of an electric field (here in a transverse direction) the crystal develops two orthogonal directions ox' and oy' (see fig. 1-a) as optical principal axes. Two waves of wavevector k_o that

are linearly polarized parallel to these directions will emerge, after traversing the crystal with a relative phase lag ϕ:

$$\phi = k_o \Delta n \, \ell \tag{2}$$

where ℓ is the length of the crystal. The electro-optic effect is usually written explicitly in the form:[6]

$$|\Delta n| = \frac{n^3}{2} \, r \, E \tag{3}$$

where r is the so-called electro-optic coefficient relating the magnitude of the birefringence to the applied electric field and n is the refractive index of the crystal. From Eq. (2) and (3) one obtains an expression for the electric field:

$$E = \left(\frac{\phi}{k_o}\right) \frac{2}{n^3 r} \frac{1}{\ell} \tag{4}$$

which can be substituted in Eq. (1) to yield the time average RF energy $\bar{W} = W/2$:

$$\bar{W} = \frac{\varepsilon_r \varepsilon_o}{n^6 r^2} \left(\frac{\phi}{k_o}\right)^2 \frac{wd}{\ell} \tag{5}$$

where w and d are the width and the thickness respectively, of the device.

The modulating electric field is applied by means of an electrical

circuit schematically shown in Fig. 1-b where R_g represents the generator's output impedance, C is the capacitance of the modulating electrodes and R a matching load in parallel. This electrical circuit can be characterized by a bandwidth Δf. It is shown in Appendix A that at the cutoff frequency Δf, the average energy stored in the electro-optic material is related to the power supplied by the RF generator through the relation:

$$P = 2\pi \Delta f \bar{W} \tag{6}$$

Combining Eqs. (5) and (6) and taking $\phi = \pi$ for 100% modulation, we obtain for the power per unit bandwidth:

$$\frac{P}{\Delta f} = \frac{\pi}{2} \left[\frac{\varepsilon_r \varepsilon_o}{n^6 r^2}\right] \lambda_o^2 \left(\frac{wd}{\ell}\right) \tag{7}$$

In Eq. (7), λ_o is the vacuum wavelength of the light to be modulated. $[\varepsilon_r \varepsilon_o / n^6 r^2]$ is homogeneous to an energy density and can be construed as a figure of merit of the electro-optical material, while the factor (wd/ℓ) depends on the geometry of the device. Notice that the apparent wavelength dependence in Eq. (7) is λ_o^2. However, the geometrical factor has been shown to be proportional to λ_o^6. Crudely, it means that one of the lateral dimensions of the crystal must be at least as large as one wavelength. Therefore, the power per unit bandwidth goes as λ_o^3. As a numerical example, let us use an average electro-optical material characterized by $\varepsilon_r \simeq 50$ and $n_r^3 \simeq 100 \times 10^{-12} = 10^{-10}$ m/volt, cut into a

rectangle of dimensions d = 5 μ, w = 20 μ and L = 1 cm. At a wavelength λ_o = 0.5 μ, Eq. (7) gives:

$$(P/\Delta f) \simeq 0.175 \text{ mW/MHz} \tag{8}$$

1.2 Magneto-optics

An expression for the power per unit bandwidth can be obtained using a very similar procedure. The energy stored in the magneto-optical material is:

$$W = \frac{1}{2} \vec{B} \cdot \vec{H}^* = \frac{1}{2} \mu_r \mu_o |H|^2 \tau \tag{9}$$

where μ_r is the relative magnetic permittivity, $\mu_o = 4\pi \times 10^{-7}$ Henry/m is the permittivity of vacuum, |H| is the magnetic field intensity and τ the volume of the crystal.

The magneto-optical interaction of interest to us is the Faraday effect, which arises when the magnetic field is applied along the direction of propagation of light as illustrated in Fig. 2-a. We consider a crystal cut in the shape of an elongated rod of radius a and length ℓ. A circular birefringence is established in the crystal. The normal modes are two opposite circularly polarized waves which propagate with different phase velocities, resulting in an effective rotation of the plane of polarization of a linearly polarized incident light. The circular birefringence $(n_+ - n_-)$ implies a relative phase lag ϕ of the

two normal modes after traversing a length ℓ of the crystal:

$$\phi = k_o (n_+ - n_-) \ell \tag{10}$$

This circular birefringence is to be paralleled with the linear birefringence caused by the electro-optic effect.

For DIAMAGNETIC AND PARAMAGNETIC materials, there exists a <u>linear</u> relation between applied magnetic field and circular birefringence:

$$n_+ - n_- = \frac{\lambda_o}{\pi} V H \tag{11}$$

where V is the so-called Verdet constant. The optical rotary power is defined by $\alpha = VH\ell$. From Eqs. (10) and (11) we get an expression for the magnetic field:

$$H = \frac{\phi}{2V} \frac{1}{\ell} \tag{12}$$

which can be substituted back into Eq. (9) to obtain an average RF energy stored $\bar{W} = W/2$.

$$W = \frac{1}{16} \left[\frac{\mu_r \mu_o}{V^2}\right] \phi^2 \left(\frac{\pi a^2}{\ell}\right) \tag{13}$$

As in the electro-optic case, we take $\phi = \pi$ for maximum modulation and obtain a power per unit bandwidth:

$$\frac{P}{\Delta f} = \frac{\pi^3}{8} \left[\frac{\mu_r \mu_o}{V^2}\right] \frac{\pi a^2}{\ell} \tag{14}$$

Comparing Eqs. (14) and (7), we notice first that the explicit wavelength dependence is not the same. However, the Verdet constant decreases with increasing λ_o,[7] roughly as $1/\lambda_o$, which restores approximately the original dependence for the power. In order to perhaps enhance the similarity between magneto-optics and electro-optics, one might want to rewrite Eq. (14) in the form:

$$\frac{P}{\Delta f} = \frac{\pi^3}{8} \left[\frac{\mu_r \mu_o}{\lambda_o^2 V^2}\right] \lambda_o^2 \left(\frac{\pi a^2}{\ell}\right) \tag{15}$$

where the quantity in brackets $[\mu_r \mu_o / \lambda_o^2 V^2]$ is now homogeneous to our energy density.

For an order of magnitude calculation, let us take a typical value of the Verdet constant of 0.02 min/Gauss-cm or 8×10^{-6} rad/Amp.[7] For a para or diamagnetic material, one can take $\mu_r \simeq 1$. For the sake of comparison, let the cross section πa^2 be equal to that of our previous electro-optic crystal (wxh = 100 μ^2).

Under these conditions, Eq. (15) gives a rather staggering $(P/\Delta f) \simeq$ 0.8 kW/MHz.

For FERRO or FERRIMAGNETIC materials such as our films, however, the numbers are quite different. Because of saturation and hysteresis effects, a simple linear relation such as Eq. (11), strictly speaking, does not exist. In spite of these complications, the problem can be

linearized as a first approximation by noting that our magneto-optic films can be saturated with an applied DC magnetic field of about H_c = 1 Oe. When saturated, our films have an optical rotary power of the order of $(\pi/2)$ rad/cm.[5] This enables us to define an effective Verdet constant V_{eff}:

$$\alpha = V_{eff} H_c \ell \tag{16}$$

Using the numbers quoted above, Eq. (16) gives:

$$V_{eff} = 5 \times 10^{3} \text{ min/Oe/cm} \tag{17}$$

compared to 2×10^{-2} min/Oe/cm in a typical paramagnetic material, a gain of 2.5×10^{5}. Our films have a $4\pi M$ of 200 Gauss, giving an initial permeability of $\mu_r = 200$. With these numbers, Eq. (14) gives:

$$(P/\Delta f) \underset{\sim}{} 2.5 \ \mu W/MHz \tag{18}$$

which compares favorably with the 175 μW/MHz which we estimated for the electro-optic case (factor of ~ 70).

1.3 Discussion

It should be emphasized that the above derivations rely on a number of simplifying assumptions.

(i) It is assumed that there is no loss mechanism other than the

dissipation of power in the matching load.

(ii) At no point was any presumption made concerning the dynamics of the modulating process. Specifically, the bandwidth is determined by the driving circuitry and not by any possible frequency limitation of the actual physical mechanism taking place inside the crystals.

(iii) The driving circuit is assumed to be designed so as to act with maximum efficiency on the material. In the electro-optics case, for example, it means that the electrodes are deposited directly against the top and bottom surfaces of the crystal. Should they be separated by a larger distance, the voltage necessary to achieve the required electric field would have to go up, increasing the power consumption.

(iv) The figures quoted above could be somewhat misleading in the sense that the power per unit bandwidth is really a figure of merit which does not reveal a complete picture of the performance of a given device. This point is perhaps best clarified by approaching the problem from a slightly different angle.

Consider the electro-optics case first, illustrated in Fig. 1. The power dissipated in the load is given by:

$$P_R = \frac{i}{2} \frac{V^2}{R} \tag{19}$$

The voltage is such that the required electric field is established in the electro-optic crystal. With the help of Eq. (4) we obtain:

$$V = E\,d = \frac{\lambda_o}{n^3}\,\frac{d}{\ell} \tag{20}$$

With the numbers used previously (λ_o = 0.5 μ, ε_r = 50, $n^3 r = 10^{-10}$ m/v, w = 20 μ, d = 5 μ and ℓ = 1 cm) Eq. (20) yields V = 2.5 volts, which gives a power dissipation P_R = 62.5 mw in a 50-Ω terminating load. The bandwidth of the circuit is

$$\Delta f = (\pi RC)^{-1} \tag{21}$$

with the capacitance given by

$$C = \varepsilon_o \varepsilon_r\, w\ell/d \tag{22}$$

Thus, Δf = 357 MHz. Dividing P_R by Δf gives the power per unit bandwidth which can be construed as a figure of merit of the device encompassing material properties of the crystal as well as circuit design parameters. In the present example, the result is 175 μW/MHz, the same figure we arrived at directly in a previous section. In fact Eqs. (19) - (22) lead directly to the expression for the power per bandwidth as written in Eq. (7).

Similarly for magneto-optics, and with reference to Fig. 2, the power dissipation is:

$$P_R = \frac{1}{2} R I^2 \tag{23}$$

Assume that the magnetic field is applied by means of a solenoid made of N turns and length ℓ tightly wound around a magneto-optic rod of radius a. The solenoid produces a magnetic field of intensity $H = NI/\ell$ while its inductance is $L = \mu_o \mu_r N^2 (\pi a^2)/\ell$. We use the following parameters: $\pi a^2 = 100\ \mu^2$, $\ell = 1$ cm, $\mu_r = 200$, $\mu_o = 4\pi\ 10^{-7}$ Henry/m and N = 10. With these numbers, the current requirement is 80 mA, giving a power consumption $P_R = 160$ mW in a 50-Ω matching load. The inductance is calculated to be 0.25 nH giving a bandwidth $\Delta f = 64$ GHz. Again, dividing P_R by Δf yields our previous result of 2.5 μw/MHz for the power per unit bandwidth. The expression for $P_R/\Delta f$ is easily obtained in explicit form. From Eq. (12), the magnetic field required for 100% modulation is $H = \pi/2V\ell$. The current necessary to create this magnetic field is $I = \pi/2NV$, giving a power consumption:

$$P_R = (\pi^2 R)/8N^2\ V^2 \tag{24}$$

The bandwidth is:

$$\Delta f = R\ell/[\pi\ \mu_o\ \mu_r\ N^2(\pi a^2)] \tag{25}$$

Indeed, dividing Eq. (24) by Eq. (25) gives exactly the result obtained in Eq. (14).

Table I summarizes our comparison of electro-optics and magneto-optics using our somewhat idealized parameters. On the basis of Table I magneto-optics appears to be a promising scheme for light modulation, particularly in the infrared where the power requirement for an electro-optic modulator increases.

A few observations should be made at this point. Notice first that in our analysis of magneto-optical modulation, although the actual power requirement exceeds that of the electro-optical device, it is the very large bandwidth of the driving circuit (due in this particular example to the very small cross section of the solenoid) which gives such an appealing figure for the power per unit bandwidth. It should also be stressed that the production of magnetic field offers more latitude with regard to circuit design than for an electric field. In the case of a solenoid, for example, the number of turns N is an additional parameter which has no counterpart in a capacitance. Note that if N is increased by a factor of 10, the power dissipation is reduced by 100, but so is the bandwidth, leaving the power per unit bandwidth unchanged.

In a practical thin film magneto-optical modulator, the necessity to periodically reverse the magnetic field makes it questionable whether a coil can be used. Pappert and Taylor[8] have recently analyzed the conventional meander line as first introduced by Tien.[4] For a periodicity of 2.4 mm, they calculate the inductance of the meander line to be 0.03 μH which corresponds to a bandwidth Δf = 500 MHz for the lumped circuit of Fig. 2-b. They also calculate that a field of $\sim$ 2 Oe is generated at the

site of the film per Ampere in the meander line. Hence, if 1 Oe is required for switching, a current of 500 mA is needed, giving a power dissipation P = 6.25 watts in a 50-ohm matching load. The power per unit bandwidth is then 12.5 mW/MHz. This figure is in good agreement with the estimate of 5 mW/MHz arrived at by Pappert and Taylor with a more refined calculation.[8]

II. DYNAMICS OF MAGNETIZATION REVERSAL

Several mechanisms can be responsible for the reversal of the magnetization in a magneto-optical material. Among the best understood processes are coherent spin rotation, which results from the torque experienced by a magnetic moment under the influence of an applied magnetic field, and domain wall motion, where a region magnetized along the direction of the applied field grows at the expense of other regions magnetized in less favorable orientations.

2.1 Coherent Rotation in a Single-Domain Sphere

Upon application of a magnetic field $\vec{H}$, a magnetization $\vec{M}$ experiences a torque $\vec{\Gamma} = \vec{M} \times \vec{B}$. The equation of motion expresses the property that the torque must be equal to the rate of change of the angular momentum. The angular momentum $\vec{g}$ and the magnetic moment $\vec{M}$ are related via the gyromagnetic ratio $\gamma = -1.76 \times 10^7$ sec^{-1} Oe^{-1}:

$$\vec{M} = \gamma \vec{g} \tag{26}$$

Thus, the equation of motion is:

$$\vec{M} \times \vec{H} = -\frac{1}{\gamma} \frac{d\vec{M}}{dt} \tag{27}$$

The solution of Eq. (27) is the well-known precession of the magnetization around the applied field at an angular frequency ω given by:

$$\omega = |\gamma| H \tag{28}$$

which corresponds to a precession frequency of:

$$f(\text{MHz}) = 2.8\ H\ (\text{Oe})$$

It is remarkable that Eq. (28) does not allow for the magnetization to ever align itself with the applied field contrary to experimental observation. The reason is the absence of a damping term. Such a term was first introduced by Landau and Lifshitz in the following form:[9]

$$\frac{d\vec{M}}{dt} = -\gamma\,(\vec{M} \times \vec{H}) - \frac{\lambda}{M^2}\,\vec{M} \times (\vec{M} \times \vec{H}) \tag{29}$$

where M represents the magnitude $|\vec{M}|$ of the magnetization. The damping term is proportional to a torque acting to tilt $\vec{M}$ toward $\vec{H}$, while the other torque $\vec{\Gamma} = \vec{M} \times \vec{H}$ still causes $\vec{M}$ to precess around $\vec{H}$. Notice that the magnetic field entering Eq. (29) is, strictly speaking, the total field which is made up of the sum of the applied field $\vec{H}_a$ and the demagnetizing field $\vec{H}_d$, which is $\vec{H}_d = -(4\pi/3)\,\vec{M}$ for a sphere. Since the demagnetizing field is collinear with $\vec{M}$, it exerts no torque on the magnetization and can, therefore, be ignored in the equation of motion.

It has been argued that the Landau-Lifshitz equation (29) suffers from shortcomings related to the unrealistic choice of two coefficients γ and λ that are independent: physically one would expect the viscosity of the medium to affect the precession as well as the rate of approach to $\vec{H}$. The fact that $d\vec{M}/dt$ increases with the damping coefficient λ is another unsatisfactory feature of equation (29).

Gilbert proposed another phenomenological equation of motion:[10]

$$\frac{d\vec{M}}{dt} = -\gamma' \vec{M} \times \vec{H} + \frac{\alpha}{M} \left(\vec{M} \times \frac{d\vec{M}}{dt}\right) \tag{30}$$

where α is dimensionless (λ was expressed in sec^{-1}). As derived in Appendix B, Eq. (30) can be transformed into:

$$\frac{d\vec{M}}{dt} = \frac{-\gamma'}{1+\alpha^2} (\vec{M} \times \vec{H}) - \frac{\alpha \gamma'}{(1+\alpha^2) M} [\vec{M} \times (\vec{M} \times \vec{H})] \tag{31}$$

The modified Gilbert equation (31) is identical in structure to the Landau-Lifshitz equation (29) with the following equivalence:

$$\alpha = \lambda/\gamma M \tag{32}$$

For large damping coefficients λ, Eq. (31) gives the physically meaningful result that both the precession frequency and the rate of approach to $\vec{H}$ slow down. It is obvious from Eqs. (29), (30) or (31) that the scalar procuct $\vec{M} \cdot (d\vec{M}/dt)$ is identically zero, indicating that the

magnitude M of the magnetization is a constant of the motion. It is in that sense that the phenomenon under consideration is a coherent rotation of all the individual spins.

As derived in Appendix C, the solution of the Gilbert equation corresponds to the magnetization "zeroing in" on the direction of the applied field while precessing around the applied field with a frequency depending on the damping coefficient. The time constant describing the rate of approach toward $\vec{H}$ is shown to be:

$$\tau = (1 + \alpha^2)/\alpha \gamma H \tag{33}$$

It is noteworthy that this time constant decreases with increasing amplitude of the applied field. Observe in Eq. (33) that the time constant τ also depends on the damping coefficient α. When $\alpha = 0$, $\tau \to \infty$, meaning that the magnetization precesses indefinitely around the magnetic field with no tendency to align itself with it. For large α, it takes a very long time for the magnetization to overcome the viscosity of the magnetic medium and approach the field. Clearly, there is an optimum situation between these two extremes corresponding to a minimum time constant. This optimum, known as critical damping, is obtained by differentiating τ with respect to α in Eq. (33) and setting $\partial \tau/\partial \alpha = 0$. Critical damping occurs when $\alpha = 1$, while underdamped and overdamped motion corresponds to $\alpha < 1$ and $\alpha > 1$, respectively. At critical damping:

$$\tau = \tau_{min} = 2/\gamma H \tag{34}$$

Using $\gamma = 1.76 \times 10^7$ sec^{-1} Oe^{-1}, and assuming that a field of 1 Oe can switch the magneto-optic crystal, Eq. (34) gives a minimum rise time of $\sim$ 100 nsec.

Recall that in the derivation of the power per unit bandwidth of a magneto-optical modulator, as outlined in Section 1.2, it was assumed that the bandwidth was determined by the driving circuit, and not by the medium itself. In view of the calculation just completed above, it is easy to see that such an assumption may be quite unrealistic in actual cases.

2.2 Coherent Rotation in a Thin Film with In-Plane Magnetization

The treatment of a sphere was particularly simple because it was assumed that the medium was magnetically isotropic, non-magnetostrictive, and we showed that the demagnetizing field played no role. In the case of a planar thin film with an in-plane magnetic easy axis, these assumptions are not justified.

The dynamical equations are obtained very simply by noting that in the isotropic case the torque $\vec{\Gamma}$ is related to the energy W by the expression:

$$|\vec{\Gamma}| = \frac{\partial W}{\partial \theta}$$

where θ is the angle between field and magnetization. By extension, when the energy depends on more than one spherical coordinate, the torque is given by:

$$\vec{\Gamma} = \frac{\partial W}{\partial \theta} \vec{i}_\phi - \frac{1}{\sin\theta} \frac{\partial W}{\partial \phi} \vec{i}_\theta \qquad (35)$$

where the unit vectors $\vec{i}_\phi$ and $\vec{i}_R$ are illustrated in Fig. 3. In the coordinate system $(\vec{i}_\phi, \vec{i}_\theta, \vec{i}_r)$, the components of the magnetization are $(0, 0, M)$, those of $d\vec{M}/dt$ are $(M \sin\theta\, d\phi/dt, M\, d\theta/dt, 0)$, and those of $\vec{M} \times d\vec{M}/dt$ are $(-M^2 d\theta/dt, M^2 \sin\theta\, d\phi/dt, 0)$.

These expressions can be substituted in the Gilbert equation written in the following form:

$$\frac{d\vec{M}}{dt} = -\gamma \vec{\Gamma} + \frac{\alpha}{M} \left(\vec{M} \times \frac{d\vec{M}}{dt}\right)$$

With the help of Eq. (35), a system of two coupled simultaneous differential equations is obtained:

$$\begin{cases} \sin\theta \dfrac{d\phi}{dt} = -\dfrac{\gamma}{M} \dfrac{\partial W}{\partial \theta} - \alpha \dfrac{d\theta}{dt} & (36\text{-a}) \\ \dfrac{d\theta}{dt} = \dfrac{\gamma}{M} \dfrac{1}{\sin\theta} \dfrac{\partial W}{\partial \phi} + \alpha \sin\theta \dfrac{d\phi}{dt} & (36\text{-b}) \end{cases}$$

which can be solved for $d\phi/dt$ and $d\theta/dt$:

$$\begin{cases} (1+\alpha^2) \dfrac{d\theta}{dt} = \dfrac{\gamma}{M} \left[\dfrac{1}{\sin\theta} \dfrac{\partial W}{\partial \phi} - \alpha \dfrac{\partial W}{\partial \theta}\right] & (37\text{-a}) \\ (1+\alpha^2) \sin\theta \dfrac{d\phi}{dt} = -\dfrac{\gamma}{M} \left[\dfrac{\partial W}{\partial \theta} + \dfrac{\alpha}{\sin\theta} \dfrac{\partial W}{\partial \phi}\right] & (37\text{-b}) \end{cases}$$

As an example, take the case of the single domain sphere considered above, with an applied field along the z axis. The energy is given by:

$$W = -MH \cos\theta + \text{isotropic demagnetizing energy.}$$

Equations (37) reduce to:

$$\frac{d\theta}{dt} = -\frac{\alpha\gamma H}{1+\alpha^2}\sin\theta \quad \text{and} \quad \frac{d|\phi|}{dt} = \frac{\gamma H}{1+\alpha^2}$$

which agree with the results derived directly in Appendix C.

Consider now a thin film in the x-y plane. The film is assumed to have a magnetic easy axis along the x-direction. With the switching field applied along this direction, the energy is given by:

$$W(\theta,\psi) = K\sin^2\phi - H M \sin\theta\cos\phi + 2\pi M^2\cos^2\theta \qquad (38)$$

In the right hand side of Eq. (38), the first term represents the uniaxial anisotropy due to the existence of the easy axis along the x-direction, the second is the magnetic energy associated with the switching field H applied longitudinally (i.e., along the easy axis), and the last term corresponds to the demagnetizing energy which arises when the magnetization is lifted out of the plane of the film.

The system of Eqs. (37) cannot be solved analytically except at the cost of approximations. The crucial argument is that the demagnetizing field is so strong - due to a large $4\pi M$ - that it forbids large excursions of the magnetization vector out of the plane of the film. It is, therefore, convenient to introduce an angle $\psi = (\pi/2) - \theta$ which remains small. Eqs. (37) can be rewritten in terms of the angles ϕ and ψ and in the approximation of small damping ($\alpha^2 << 1$):

$$\begin{cases} -\frac{d\psi}{dt} = \frac{\gamma}{M}\left[\frac{\partial W}{\partial \phi} + \alpha \frac{\partial W}{\partial \psi}\right] & (39\text{-a}) \\ -\frac{d\phi}{dt} = \frac{\gamma}{M}\left[-\frac{\partial W}{\partial \psi} + \alpha \frac{\partial W}{\partial \phi}\right] & (39\text{-b}) \end{cases}$$

with $W(\phi, \psi)$ given by:

$$W = K \sin^2\phi - H M \cos\psi \cos\phi + 2\pi M^2 \sin^2\psi \qquad (40)$$

α is assumed small enough so that in Eq. (39-b) the second term in the bracket can be neglected. This is not too stringent a condition since $\partial W/\partial\psi$ contains the demagnetizing field which is much stronger than either the applied or the anisotropy field. Thus Eq. (39-b) can be approximated by its undamped form:

$$\frac{d\phi}{dt} = \frac{\gamma}{M} \frac{\partial W}{\partial \psi} \qquad (41)$$

which can be differentiated with respect to time:

$$\frac{d^2\phi}{dt^2} = \frac{\gamma}{M} \frac{\partial^2 W}{\partial \psi^2} \frac{\phi\psi}{dt} \qquad (42)$$

Substitution of Eqs. (39-a) and (41) into (42) leads to a second-order differential equation in ϕ. Using the relation $\partial^2 W/\partial\psi^2 \simeq 4\pi M^2$ obtained from Eq. (40), the result is:

$$\frac{d^2\phi}{dt^2} + 4\pi\gamma\alpha M \frac{d\phi}{dt} + 4\pi\gamma^2 \frac{\partial W}{\partial \phi} = 0 \qquad (43)$$

Recalling that α was defined as $\alpha = \lambda/\gamma M$, Eq. (43) is identical to that derived by Smith.[11] The partial derivative $\partial W/\partial\phi$ has the form:

$$\frac{\partial W}{\partial \phi} = M\ (H_K \cos\phi + H)\ \sin\phi \tag{44}$$

where $H_K = 2K/M$ is the effective anisotropy field. In the approximation of small angle ϕ, $\sin\phi \simeq \phi$ and Eq. (43) can be linearized:

$$\frac{d^2\phi}{dt^2} + 4\pi\gamma\alpha M\ \frac{d\phi}{dt} + 4\pi\gamma^2 M\ (H_K+H)\ \phi = 0 \tag{45}$$

The solution corresponds to oscillations of frequency ω such that:

$$(\omega/2\pi)^2 = \gamma^2\ \pi^{-1}\ M\ (H_K+H) - (\alpha\gamma M)^2 \tag{46}$$

These oscillations decay with a time constant τ:

$$\tau = (2\pi\gamma\alpha M)^{-1} \tag{47}$$

The motion can be understood as follows. The field applied along the easy axis exerts at first a torque that tends to lift the magnetization out of the film's plane. This process creates a demagnetizing field normal to the film which, in turn, causes an in-plane rotation of the magnetization. The switching time can be estimated by neglecting the oscillatory term in the dynamical equation, which then reduces to:

$$\alpha \frac{d\phi}{dt} + \gamma H \left[\frac{H_K}{H} \cos\phi + 1\right] \sin\phi = 0 \qquad (48)$$

This corresponds to the so-called viscous flow approximation as discussed by Smith.[11] Eq. (48) enables us to define a time constant τ_s:

$$\tau_s = \frac{\alpha}{\gamma H} = \frac{\lambda}{\gamma^2 MH} \qquad (49)$$

As a numerical example, using $4\pi M = 200$ Gauss, $\lambda = 20$ MHz (this order of magnitude will be justified later) and $H = 1$ Oe, we get $\tau_s = 4$ nsec. Notice again in Eq. (24) that the switching time decreases with increasing field as well as increasing $4\pi M$.

2.3 Dynamics of Wall Motion

Consider a Bloch wall between two regions of antiparallel magnetization, as illustrated in Fig. 4-a. It is assumed that the wall energy W_w is some function of the position s such as the one shown in Fig. 4-b. That W_w should depend on s is attributed to the fact that domain walls are influenced by impurities, dislocations, and other irregularities which have a certain spatial distribution throughout a crystal. Upon application of a magnetic field H in the +z direction, the region of parallel magnetization grows at the expense of the other one, pushing the wall by a distance s, since this leads to a lowering of the magnetostatic energy W_H by an amount:

$$W_H = -2M H s \qquad (50)$$

per unit area of the wall. The factor of 2 comes about because the magnetization is reversed by 2xM. The wall moves to a new equilibrium position which minimizes the total energy $W_w + W_H$. This occurs where

$$\frac{\partial W}{\partial s} = 2 M H \tag{51}$$

With increasing field, the wall moves further out until it reaches the position s, corresponding to the inflection point of $W_w(s)$. With a small additional field, the equilibrium condition (51) can no longer be satisfield in the vicinity of s, and the wall suddenly moves to the position s_2 where Eq. (51) can again be verified. This discontinuity is usually referred to as a Barkhausen jump. It is irreversible in the sense that upon removal of the field, the wall does not come back to its original position.

The entire sample will become uniformly magnetized. The field is strong enough to overcome the largest gradient $\frac{\partial W}{\partial s}$. Thus, one defines a coercive field H_c:

$$H_c = \frac{1}{2M} \left[\frac{\partial W}{\partial s}\right]_{max} \tag{52}$$

By contrast, if magnetization reversal takes place by coherent rotation, the coercive field would be equal to the anisotropy field H_K.

In view of the above, a domain wall executing small reversible displacements can be assimilated to a harmonic oscillator in a potential

wall described by Fig. 4-b. The equation of motion is:[12]

$$m_w \frac{d^2 s}{dt^2} + \beta \frac{ds}{dt} + k s = 2 M H \tag{53}$$

where m_w is the effective mass per unit area of the wall, β, a damping coefficient, and k describes the restoring force. For a wall other than Bloch-type, the numerical coefficient appearing on the right hand side of Eq. (53) might be different, but the basic dynamical behavior remains the same.

For large irreversible displacements under the influence of a field $H > H_c$, one can write an approximate equation of motion by neglecting the effective mass m_w:

$$\beta \frac{ds}{dt} = 2 M (H - H_c) \tag{54}$$

Eq. (54) amounts to considering the crystal simply as a viscous medium. The motion of a wall is characterized by a time constant τ:

$$\tau = \frac{\beta}{2M(H-H_c)} \tag{55}$$

while the actual switching time depends on the distance over which the wall has to move.

Domain wall motion can be thought of as rotation of the magnetization within the wall, creating a disturbance which propagates down the crystal. Because of the "sequential" nature of the process, magnetization

reversal by domain wall motion is expected to be slower than by coherent rotation over the entire sample.

Therefore, the performance of a thin film magneto-optic modulator will be determined largely by the type of physical mechanism that is responsible for the switching.

III. EXPERIMENTS IN $Gd_{.5}Y_{2.5}Ga_1Fe_4O_{12}$ WAVEGUIDES

Our experimental work was divided along the following lines, listed in chronological order:

- Waveguiding properties on garnet thin films.
- TE → TM mode conversion experiments.
- Domain structure of the films.
- Electromagnetic sensing of resonant oscillations of the magnetization.
- Optical switching speed.

3.1 Summary of Earlier Results

3.1.1 Garnet Waveguides:

Thin films of $(Gd_{.5}Y_{2.5}Ga_1Fe_4)O_{12}$ grown by liquid phase epitaxy on [111] gadolinium gallium garnet disks at our laboratory were found to be suitable for waveguiding at a wavelength of 1.15 μm. Thicknesses ranged from 5 to 10 μm and the refractive index was typically 2.14. The attenuation coefficient, due primarily to absorption by impurities, was measured to be about 7 dB/cm. Some magnetic properties were also measured. The films had a $4\pi M$ of 200 to 250 Gauss, a coercive field from 0.5 to 1 Oe and an in-plane anisotropy field in the range of 3 to 6 Oe.[13]

3.1.2 Mode Conversion Experiments:

Efficient TE $\rightleftarrows$ TM mode conversion was observed in these films by

spatially periodic reversal of the in-plane magnetization in order to compensate for the phase mismatch between TE and TM modes. This was accomplished by means of either (i) a conventional electrical meander line or (ii) a novel scheme involving a magnetized periodic Permalloy structure in close vicinity of the film. During the course of these experiments, we determined that the optical rotary power of our films ranged from 100 to 150 deg/cm, making complete conversion possible over an interaction length of $\sim$ 1 cm.[14]

3.1.3 Domain Structure:

When examined between crossed analyzer and polarizer, our films display a stripe pattern of low, but nonetheless, observable contrast. This indicates that the magnetization is not completely in-plane, and that at low field, the films tend to break up into domains. The field intensity required to annihilate these domains is a function of orientation and reveals the three-fold symmetry of the [111] plane of the film. Furthermore, we showed how the domain pattern is influenced by the periodic Permalloy structure and how it directly correlates with the observed conversion efficiency.[15]

3.1.4 Resonant Oscillations of the Magnetization:

By electromagnetic sensing via a balanced half-turn pick-up loop, free oscillations of the magnetization, of the type discussed in Section 2.2, were observed, ranging in frequency from 200 to 900 MHz depending on bias magnitude and direction.[16]

These oscillations were also present when the samples were driven at RF frequencies. They typically decayed over a period of about 10 nsec, giving a damping coefficient $\lambda \approx 18$ MHz. This agrees well with figures of between 5 and 20 MHz quoted by Tien in his films.[17]

3.1.5 Optical Switching Speed:

Samples were placed inside strip lines in which current pulses were launched. It was found that the speed of the optical response depended very strongly on the amplitude of the switching field. For a sample influenced by a periodic Permalloy structure, the optical rise time decreased from 10 μsec to 60 nsec as the magnetic field pulse went from 0.5 Oe to 5 Oe. We offered evidence that this behavior was not due to the Permalloy, but rather, was intrinsic to the garnet films.[18]

3.2 Recent Results

3.2.1 Current Driven Permalloy:

In our 5th Quarterly Report, we proposed a structure designed to reduce the current required for modulation. The scheme, illustrated in Fig. 5, consists of a garnet waveguide protected by a layer of SiO_2 ($\sim$ 3000 Å thickness), on top of which Permalloy is deposited. The structure is then electroplated with copper and a periodic structure of appropriate periodicity is then etched photolithographically into the conducting materials (copper and Permalloy). A small current launched in the copper lines should magnetize the Permalloy which, in turn, should influence the magneto-optic waveguide.

We did fabricate such a device and we have measured its performance. The structure had 10 periods with a periodicity of 40 mils. The inductance of the device was measured to be 0.016 μH. The current requirement was indeed considerably reduced, since we observed optical modulation with only 200 to 500 mA, as compared with the 10 Amps or more that were necessary in the strip lines used in earlier experiments. Increasing the current to about 750 mA was detrimental to the conversion efficiency, because the magnetic field created by the current would start overriding that created by the Permalloy, thereby destroying the periodic reversal of magnetization. We proceeded to feed a constant current of 200 mA peak and increase the frequency. The amplitude of the optical signal dropped steadily between 100 KHz and 1 MHz as shown in Fig. 6. Furthermore, it was observed that in the same range of frequencies, the phase of the optical signal gradually fell behind the driving field from 0 to $-\pi$ as shown in Fig. 7. More quantitative data on the phase lag are shown in Fig. 8. It is remarkable that the data presented in Figs. 6 and 8 can be fitted to the equation of motion of a harmonic oscillator as discussed in Section 2.3 in connection with reversible domain wall displacement:

$$\frac{d^2s}{dt^2} + \kappa \frac{ds}{dt} + \omega_o^2 = F e^{i\omega t} \tag{56}$$

where $\kappa = \beta/m_w$, β and m_w defined in Eq. (53).

The solution to Eq. (1) is $x = |A| e^{j\phi} e^{j\omega t}$ with:

$$|A| \propto [(\omega_o^2 - \omega^2)^2 + \kappa^2 \omega^2]^{1/2} \qquad (57)$$

and

$$\phi = \tan^{-1} [\kappa \omega/\omega^2 - \omega_o^2]$$

The best fit between experimental data and Eq. (57) is obtained for $\omega_o = 2.5 \times 10^{+6}$ sec^{-1} and $\kappa = 1.25 \times 10^7$ sec^{-1}, as shown by the curves of Figs. 6 and 8. This observation strongly suggests that the optical modulation observed here is due to reversible domain wall motion. Another indication pointing toward domain wall motion is the fact that if the current is increased to about 500 mA, the optical signal becomes quite unstable, displaying considerable jitter characteristic of Barkhausen jumps. Driving the device with a fast current pulse of 300 mA produced an optical signal with a rise time of 5 μsec.

3.2.2 Meander Line:

Motivated by the desire to lay to rest any lingering suspicion that the Permalloy might be to blame, we carried out switching experiments using a meander line of the type used by Tien.[4] With 10 periods and a periodicity of 40 mils, we obtained an inductance of 0.16 μH, giving an electrical rise time L/R of about 3 nsec.

By applying fast current pulses, we found here again that the rise time of the optical signal depends on the pulse amplitude. The results are shown in Fig. 9 for two different samples. The apparent saturation at around 4 nsec is due to the bandwidth limitation of the photomultiplier. Fig. 10 shows the shape of the optical signal.

Sample #851 is the one on which we prevlously carried out pulsed experiments with a Permalloy structure placed in a strip line. With this set-up, the magnetic field to current calibration was 0.5 Oe/ Amp. In the present configuration, by superposing a known external field to cancel the effect of the meander line, we determined that a field of about 10 Oe/Amp is produced at the site of the sample. Hence we can plot on a single diagram the rise time vs. field pulse amplitude obtained from both experiments. The result is shown in Fig. 11. We conclude that the film behaves in an essentially similar manner whether it is switched via a meander line or a Permalloy structure. The difference in rise time is merely due to the different range in field pulse amplitude. For purposes which will become clear in the next section, Fig. 12 also shows $1/\tau$ vs. switching field.

3.2.3 Switching Mechanism:

The fact that the rise time decreases with increasing field amplitude is not only in qualitative agreement with theory, but has, in fact, been observed in ferromagnetic materials by several other workers. We refer, for example, to the experiments of Conger and Essig[19], Gyorgy[20], Olson and Pohm[21], Hagedorn [22], and Dietrich et al [23], among others. The results of Dietrich et al in thin Permalloy films are reproduced in Fig. 13, where the branches of small and large slopes are assigned to domain wall motion and coherent rotation, respectively, occurring simultaneously. On the basis of Fig. 12, we surmise that a gradual transition from one regime to the other takes place with increasing driving field. The data of Olson and Pohm[21] (see their figures 5, 6, and 7) and

those of Hagedorn[22] (his Fig. 1) in particular look remarkably similar to ours.

It is generally agreed that magnetization switching by coherent rotation prevails at fields larger than the anisotropy field $H_K = 2K/M$. Below this value, and down to the coercive field, the most likely process is irreversible domain wall motion, with a possible transition in between by way of incoherent rotation. The fact that in our films the anisotropy field is substantially larger than the coercive field suggest that there exists a range (roughly from 1 to 5 Oe) where domain wall motion should be predominant. In our experiment with current driven Permalloy, a current of 200 mA generated a field of 1.2 Oe, barely above the coercive field and much less than the anisotropy field. Hence it is no surprise that modulation was found to be due to domain wall motion. Similarly, the strip line we used in our earlier experiments could generate, with a current of 10 Amps, a field of 5 Oe, not quite enough to penetrate in the region where coherent rotation might become important. The advantage of the meander line is a more favorable current to magnetic field conversion ratio.

IV. CONCLUSIONS

Conventional calculations of the power per unit bandwidth are based on the assumption that the physical mechanism responsible for modulation is fast enough for the bandwidth to be determined by the driving circuit alone. It is also generally assumed that the frequency response of the modulating process is independent of the amplitude of the driving force.

While these assumptions may well be justified for an electro-optical modulator, they usually are not in a magneto-optical device. The dynamical behavior of an assembly of spins placed in a magnetic field depends very much on the amplitude of this field. This often overlooked property plays, in fact, a very important role in determining the performance of a m-o modulator. Whether magnetization reversal takes place by coherent rotation or domain wall motion, theoretical models show that the time constant of the process decreases with increasing amplitude of the switching field. Without speculation as to which particular mechanism is predominant in a given situation, experiments show the switching time to obey a relation of the type:

$$\frac{1}{\tau} = F(H) \tag{58}$$

where $F(H)$ is a monotonically increasing function of the amplitude H of the modulating field. It is thus quite possible that for a particular switching field the bandwidth of a device might be determined by the material itself, rather than by the driving circuit.

Hence, in order to realistically assess the performance of a m-o modulator, the first information necessary is the knowledge of the actual functional dependence of the switching time on field amplitude, i.e., a relation of the type of Eq. (58).

If the desired bandwidth is Δf, it corresponds to a rise time $\tau \underline{\sim} 0.3/\Delta f$, which implies that the switching field has to be larger

than or equal to a minimum value given by inverting Eq. (58):

$$H_{min} = F^{-1} (\Delta f) \tag{59}$$

The magnetic field is proportional to the current flowing in the driving circuit (coil, meander line, etc.):

$$H = K I \tag{60}$$

Eq. (60) gives a minimum current requirement of:

$$I_{min} = [F^{-1} (\Delta f)]/K \tag{61}$$

which, in turn, gives a power consumption:

$$P = \frac{1}{2} R I_{min}^2 = \frac{R}{2K^2} [F^{-1} (\Delta f)]^2 \tag{62}$$

where the function in brackets characterizes the frequency response of the magneto-optic sample, while the coefficient K is a measure of the "efficiency" of the driving circuit.

From an engineering point of view, the best choice of driving circuit will be one with maximum coefficient K and with bandwidth just equal to the desired Δf.

As an example, let us consider our sample #851 in conjunction with the meander line, the inductance of which was measured to be 0.16 μH,

corresponding to a rise time $\tau = R/L = 3$ nsec or a bandwidth $\Delta f = 0.3/\tau =$ 100 MHz.

Let us first use the conventional analysis as outlined by Pappert and Taylor, where the basic assumption is that the rise time intrinsic to the material is much smaller than the 3 nsec characteristic of the driving circuit. The current requirement is such that the magnetic field be equal to the coercive field H_c. For Sample #851, $H_c \underset{\sim}{\sim} 1$ Oe. The meander line was determined experimentally to be capable of generating $\sim$ 10 Oe per Ampere, i.e., K = 10 Oe x Amp^{-1}. Thus it should take a current of 0.1 Amp for switching. The power consumption in a 50-Ω matching load would be:

$$P = \frac{1}{2} R I^2_{min} = 250 \text{ mW}$$

giving a power per unit bandwidth of:

$$\frac{P}{\Delta f} = 2.5 \text{ mW/MHz.}$$

In actuality, we now know that the switching speed of the material depends on the amplitude of the switching field. By extrapolation of Fig. 9, a switching speed of 3 nsec would require a magnetic field of $\sim$ 14 Oe, which translates into a current of 1.4 Amp in the meander line. The power consumption becomes $P = \frac{1}{2} R i^2 = 50$ watts, giving a power per unit bandwidth of 500 mW/MHz, rather than 2.5 mW/MHz.

In view of the numbers quoted above, it is clear that our films,

as they are available to us at the present time, can hardly compare with a thin film modulator using the electro-optic effect. We have seen that a RF power of 50 Watts is required to drive them at 100 MHz. This unappealing figure is due primarily to material limitations, it reflects the fact that fields in excess of 10 Oe are required for a switching speed faster than 5 nsec.

It is interesting to compare our results with those of Tien et al. Although the power per unit bandwidth was not discussed as such, some numbers can be inferred from their data. The best experimental result quoted in Ref. 17 is a modulation ratio slightly above 50% at 300 MHz for a switching field of 6 Oe. With a meander line rated at 6 Oe/Amp, the power consumption is approximately 25 Watts, giving a power per unit bandwidth of 85 mW/MHz. This somewhat better result can be attributed to the following facts. Tien's films are quoted as having a coercivity H_c 0.1 to 0.3 Oe and an in-plane anisotropy field $H_K \simeq 1.2$ Oe. By contrast, our samples have H_c = 0.5 to 1 Oe and H_K = 3 to 5 Oe. On the premise that coherent rotation prevails at driving fields larger than H_K, our films require more current to be operated in this regime.

In summary, although there is room for improvement from the point of view of material properties, magneto-optics does not appear competitive with electro-optics as a scheme for constructing wideband, low-power, thin films integrated optical modulators.

APPENDIX A

Referring to Fig. 1-b, the impedance of the device (capacitor in parallel with matching load) is $Z = R/(1+j\ RC\omega)$. The voltage V across the crystal is therefore given by:

$$\frac{V}{V_g} = \frac{R/(1+j\ RC\omega)}{R_g + R/(1+j\ RC\omega)} = \frac{1}{2+j\ RC\omega} \qquad (A\text{-}1)$$

where we have made $R = R_g$ for impedance matching. The bandwidth $\Delta\omega$ is defined as the frequency at which the voltage V drops by a factor $1/\sqrt{2}$ compared to its DC value:

$$\Delta\omega = 2/RC \qquad (A\text{-}2)$$

The average energy stored in the capacitor is $\bar{W} = (1/4)\ CV$, giving a reactive power P_x at the angular frequency $\Delta\omega$:

$$P_x(\Delta\omega) = \frac{\bar{W}}{\text{period}} = \frac{\Delta\omega}{2\pi}\bar{W} = \frac{\Delta\omega}{8\pi}\ CV^2 \qquad (A\text{-}3)$$

while the power dissipated in the matching load is:

$$P_R = \frac{1}{2}\ \frac{V^2}{R} \qquad (A\text{-}4)$$

From Eqs. (A-3) and (A-4) we obtain:

$$P_R/P_x(\Delta\omega) = 2\pi \qquad (A\text{-}5)$$

Similarly for the magneto-optics case, we refer to Fig. 2-b. The current is given by:

$$I = \frac{V_g}{2R + j\,L\omega} \qquad A\text{-}6)$$

where again we have made $R = R_g$. The bandwidth is defined as the frequency at which the current drops by $1/\sqrt{2}$ compared to its DC value:

$$\Delta\omega = 2R/L \qquad (A\text{-}7)$$

The average energy stored in the inductance is $\bar{W} = (1/4)\ L\ I^2$ which corresponds to a reactive power P_x at the angular frequency $\Delta\omega$:

$$P_x(\Delta\omega) = \frac{\Delta\omega}{8\pi} L\ I^2 \qquad (A\text{-}8)$$

while the power dissipated is $P_R = \frac{1}{2} R\ I^2$, which again leads to the relation:

$$P_R/P_x(\Delta\omega) = 2\pi \qquad (A\text{-}9)$$

While the power dissipated is independent of frequency, the reactive power stored in the active material increases with it. At the cutoff frequency Δf, the power consumption is equal to 2π times the RF power stored.

APPENDIX B

The Gilbert equation reads:

$$\frac{d\vec{M}}{dt} = - \gamma \, (\vec{M} \times \vec{H}) + \frac{\alpha}{M} \, (\vec{M} \times \frac{d\vec{M}}{dt}) \tag{B-1}$$

Taking the vector product $\vec{M} \times \frac{d\vec{M}}{dt}$, one obtains:

$$\vec{M} \times \frac{d\vec{M}}{dt} = - \gamma \, [\vec{M} \times (\vec{M} \times \vec{H})] + \frac{\alpha}{M} \, [\vec{M} \times (\vec{M} \times \frac{d\vec{M}}{dt})] \tag{B-2}$$

The quantity in the second bracket can be transformed using the triple vector product identity:

$$M \times (\vec{M} \times \frac{d\vec{M}}{dt}) = (\vec{M} \cdot \frac{d\vec{M}}{dt}) \, \vec{M} - M^2 \frac{d\vec{M}}{dt} = - M^2 \frac{d\vec{M}}{dt} \tag{B-3}$$

since, obviously, $\vec{M} \cdot \frac{d\vec{M}}{dt} = 0$.

Eq. (B-2) becomes:

$$\vec{M} \times \frac{d\vec{M}}{dt} = - \gamma \, [\vec{M} \times (\vec{M} \times \vec{H})] - \alpha \, M \frac{d\vec{M}}{dt}$$

which can be substituted back into Eq. (B-1) to give after rearrangement:

$$(1 + \alpha^2) \frac{d\vec{M}}{dt} = - \gamma \, (\vec{M} \times \vec{H}) - \frac{\alpha\gamma}{M} \, [\vec{M} \times (\vec{M} \times \vec{H})] \tag{B-4}$$

which has the same structure as the Landau-Lifshitz equation with the

following correspondence:

$$\gamma \rightarrow \gamma/(1+\alpha^2)$$

$$\lambda = \alpha\gamma M$$

APPENDIX C

Assume that a magnetic field $\vec{H}$ is applied along the +z direction. The motion of the magnetization is described by the Gilbert equation:

$$\frac{d\vec{M}}{dt} = -\gamma\,(\vec{M} \times \vec{H}) + \frac{\alpha}{M}\,(\vec{M} \times \frac{d\vec{M}}{dt}) \qquad \text{(C-1)}$$

where M represents the magnitude of $\vec{M}$ at saturation. In a cartesian coordinate system, Eq. (C-1 decomposes into:

$$\frac{dM_x}{dt} = -\gamma H M_y + \frac{\alpha}{M} M_y \frac{dM_z}{dt} - \frac{\alpha}{M} M_z \frac{dM_y}{dt}$$

$$\frac{dM_y}{dt} = \gamma H M_x + \frac{\alpha}{M} M_z \frac{dM_x}{dt} - \frac{\alpha}{M} M_x \frac{dM_z}{dt} \qquad \text{(C-2)}$$

$$\frac{dM_z}{dt} = \frac{\alpha}{M} M_x \frac{dM_y}{dt} - \frac{\alpha}{M} M_y \frac{dM_x}{dt}$$

The last three relations constitute a system of three inhomogenous linear equations which can be solved for dM_x/dt, dM_y/dt and dM_z/dt.

$$\begin{cases} (1+\alpha^2)\,\dfrac{dM_x}{dt} = -\gamma H\,[M_y + \alpha M_x M_z/M] & \text{(C3-a)} \\ (1+\alpha^2)\,\dfrac{dM_y}{dt} = \gamma H\,[M_x - \alpha M_y M_z/M] & \text{(C3-b)} \\ (1+\alpha^2)\,\dfrac{dM_z}{dt} = +\gamma H(\alpha/M)\,[M_x^2 + M_y^2] & \text{(C3-c)} \end{cases}$$

M_x, M_y and M_z subject to the condition:

$$M_x^2 + M_y^2 + M_z^2 = M^2 \qquad \text{(C-4)}$$

The magnetization components can be expressed in terms of spherical coordinates (see Fig. 3):

$$\begin{cases} M_x = M \sin\Theta \cos\phi \\ M_y = M \sin\Theta \sin\phi \\ M_z = M \cos\Theta \end{cases} \qquad \text{(C-5)}$$

where Θ (t) and ϕ(t) are two independent variables that are functions of t. Substituting Eq. (C-5) into (C3-A), for example, and dividing by $\sin\Theta \cos\phi$, we obtain:

$$(1 + \alpha^2)\,\left[-\tan\phi\,\frac{d\phi}{dt} + \frac{1}{\tan\Theta}\,\frac{d\phi}{dt}\right]$$

$$= -\gamma H \tan\phi - \alpha\gamma H \cos\Theta \qquad \text{(C-6)}$$

Since ϕ and Θ are independent variables, the terms containing ϕ and Θ

respectively, on each side of Eq. (C-6) must be equalized. Doing so leads to the two differential equations:

$$(1+\alpha^2)\,\frac{d\phi}{dt} = \gamma H \tag{C7-a}$$

$$\frac{d\theta}{\sin\theta} = -\frac{\alpha\gamma H}{1+\alpha^2}\,dt \tag{C7-b}$$

Eq. (C7-a) indicates that the angular velocity $d\phi/dt$ is a constant of the motion:

$$\frac{d\phi}{dt} = \text{constant} = \omega = \frac{\gamma H}{1+\alpha^2} \tag{C-8}$$

The precession frequency is slowed down by the damping α.

The integration of Eq. (C7-b)

$$\int_{\theta_o}^{\theta} \frac{d\theta}{\sin\theta} = -\frac{\alpha\gamma H}{1+\alpha^2}\,t$$

which can be obtained directly from Eq. (C3-c) leads to the solution:

$$\tan\frac{\theta}{2} = \left(\exp -\frac{t}{\tau}\right)\tan\frac{\theta_o}{2} \tag{C-9}$$

with the time constant τ given by:

$$\tau = \frac{1+\alpha^2}{\alpha|\gamma H|} \tag{C-10}$$

REFERENCES

1) F. S. Chen, IEEE Proc. 58, 1440 (1970).

2) L. K. Anderson, Appl. Phys. Lett. 1, 44 (1962).

3) J. T. Hanlon and J. F. Dillon, Jr., J. Appl. Phys. 36, 1269 (1965).

4) P. K. Tien, R. J. Martin, R. Wolfe, R. C. LeCraw, and S. L. Blank, Appl. Phys. Lett. 21, 394 (1972).

5) S. C. Tseng, A. R. Reisinger, E. A. Giess, and C. G. Powell, Appl. Phys. Lett. 24, 265 (1974).

6) J. P. Kaminow and E. H. Turner, IEEE Proc. 54, 1374 (1966).

7) Condon and Odishaw, Handbook of Physics, (McGraw-Hill, 2nd ed., (1967), 6-119.

8) R. A. Pappert and H. F. Taylor, Report #TR 1924, Final Technical Report (June 1974).

9) L. Landau and E. Lifshitz, Physik. Z. Sovietunion 8, 153 (1935).

10) T. L. Gilbert, Phys. Rev. 100, 1243 (1955).

11) D. O. Smith, J. Appl. Phys. 29, 264 (1958).

12) R. W. Shaw, J. W. Moody and R. M. Sandfort, J. Appl. Phys. 45, 2672 (1974).

13) A. R. Reisinger, S. C. Tseng, 1st Quarterly Technical Report (June 1973).

14) 2nd " " " (Sept. 1973)

15) 3rd " " " (May 1974)

16) J. M. White and S. C. Tseng 4th " " " (June 1974)

17) P. K. Tien, D. P. Schinke and S. L. Blank, J. Appl. Phys. 45, 3059 (1974).

18) A. R. Reisnger, S. C. Tseng 5th Quarterly Technical Report (July 1974)

19) R. L. Conger and F. C. Essig, Phys. Rev. 104, 915 (1956).

20) E. M. Gyorgy, J. Appl. Phys., 28, 1011 (1957).

21) C. D. Olson and A. V. Pohm, J. Appl. Phys. 29, 274 (1958).

22) F. B. Hagedorn, J. Appl. Phys., 30 2545 (1959).

23) W. Dietrich, W. E. Proebster and P. Wolf, IBM J. Res. & Develop. 189 (1960).

FINANCIAL STATEMENT

Contract N00014-73C-0256

Total Amount Contract	Inception to Date	Unexpended Funds
$148,578.00	$148,578.00	None

	ELECTRO-OPTICS	MAGNETO-OPTICS
Wavelength	$\lambda_o = 0.5$ μm	$\lambda_o = 1.15$ μm
Geometry	$\ell = 1$ cm	$\ell = 1$ cm
	$w = 20$ μm, $d = 5$ μm, $wd = 100$ μm^2	$a = 5.6$ μm → $\pi a^2 = 100$ μm^2
Electromagnetic Quantities	$E = 5 \times 10^5$ V/m	$H = 1$ Oe $= 80$ Amp/m
	$V = 2.5$ Volts	$I = 80$ mA with $N = 10$ turns
Power	$P_r = V^2/2R = 62.5$ mW	$P_r = RI^2/2 = 160$ mW
Reactance	$C = \epsilon_r \epsilon_o wd/\ell = 18$ pFd	$L = \mu_r \mu_o N^2 \pi a^2/\ell = 0.25$ nH
Bandwidth	$\Delta f = 1/\pi RC = 350$ MHz	$\Delta f = R/\pi L = 64$ GHz
$P_r/\Delta f$	175 μW/MHz	2.5 μW/MHz

Table 1. Comparison of electro-optics and magneto-optics under idealized conditions. It is assumed that the bandwidth is determined by the driving circuit alone, and not by the physical process involved

- Figure Captions -

Fig. 1. Electro-optic modulator. Experimental configuration (a) and equivalent driving circuit (b).

Fig. 2. Magneto-optic modulator. Experimental configuration (a) and equivalent driving circuit (b).

Fig. 3. Magnetization in spherical coordinates.

Fig. 4. Domain wall displacement in applied magnetic field.

Fig. 5. Configuration of integrated magneto-optical modulator. Current in the copper lines magnetizes the Permalloy which in turn interacts with the Garnet film.

Fig. 6. Frequency response of the device shown in Fig. 5 driven with 400 mA peak to peak.

Fig. 7. Illustrating the phase lag between optical signal and driving current for the device shown in Fig. 5. Frequencies are 10 kHz (a), 500 kHz (b) and 1 MHz (c).

Fig. 8. Phase lag of optical signal relative to driving current vs frequency for device shown in Fig. 5.

Fig. 9. Rise time of optical signal in two typical samples driven by a current pulse in a meander line.

Fig. 10. Optical response in sample #526. Horizontal scale is 5 nsec/cm. Current pulse amplitude was 4 Amps.

Fig. 11. Optical signal rise time vs amplitude of magnetic field pulses for sample #851 driven either by Permalloy in 50-Ω strip line or by a meander line.

Fig. 12. Inverse switching time in μsec^{-1} vs amplitude of magnetic field pulse.

Fig. 13. Results of Dietrich et al, from ref. 23. Notice the trend similar to our Fig. 12.

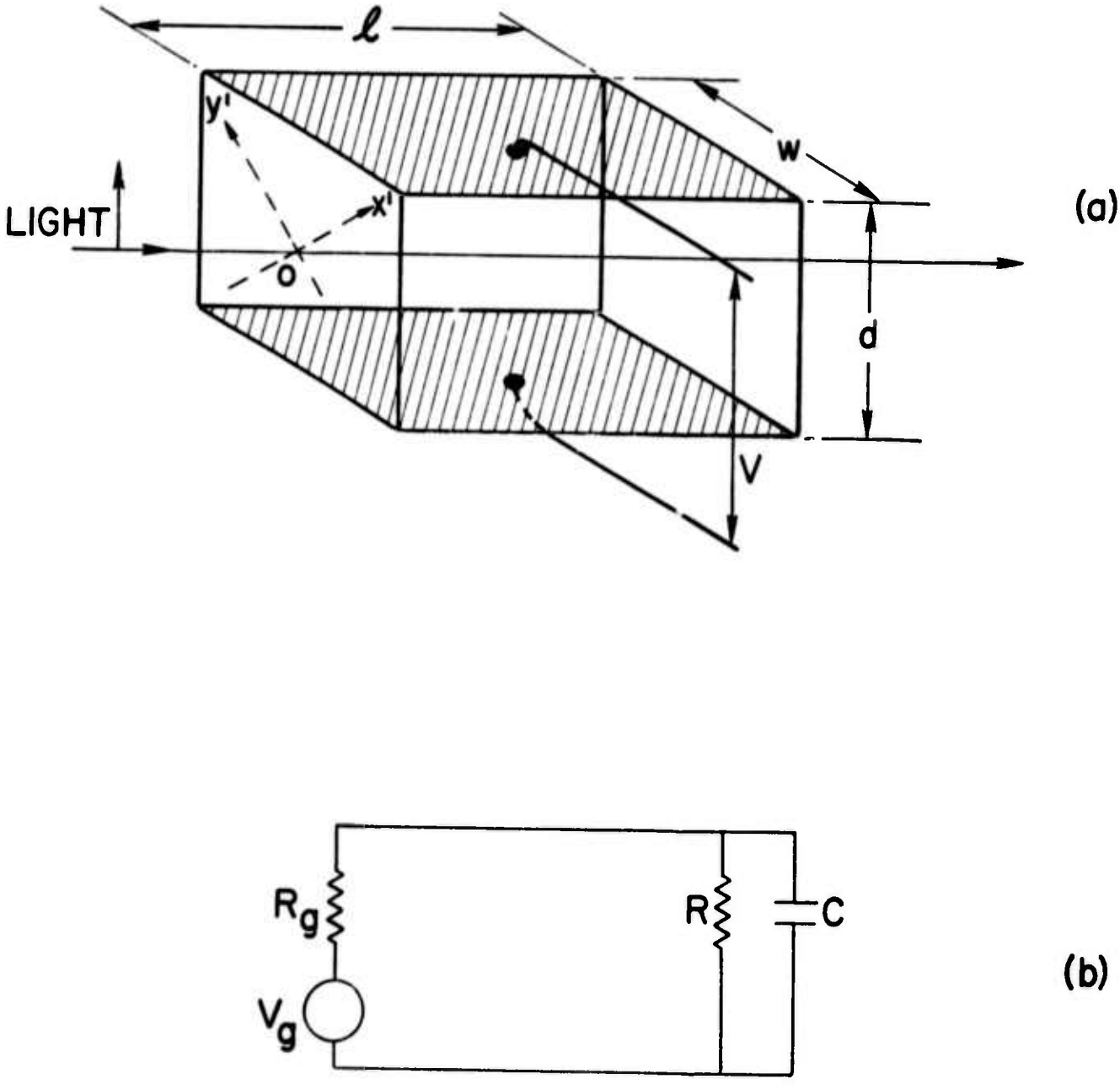

Fig. 1. Electro-optic modulator. Experimental configuration (a) and equivalent driving circuit (b).

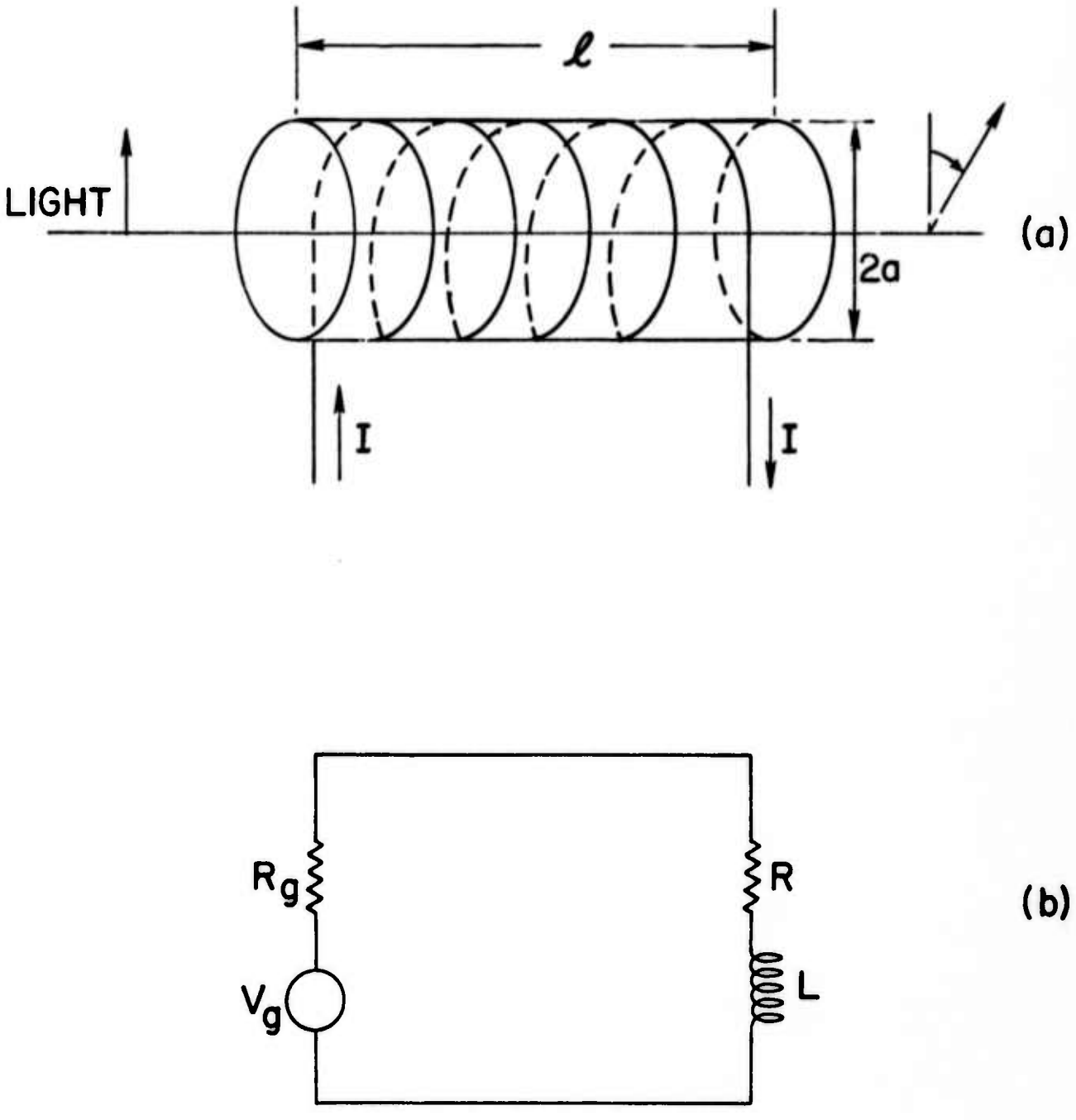

Fig. 2. Magneto-optic modulator. Experimental configuration (a) and equivalent driving circuit (b).

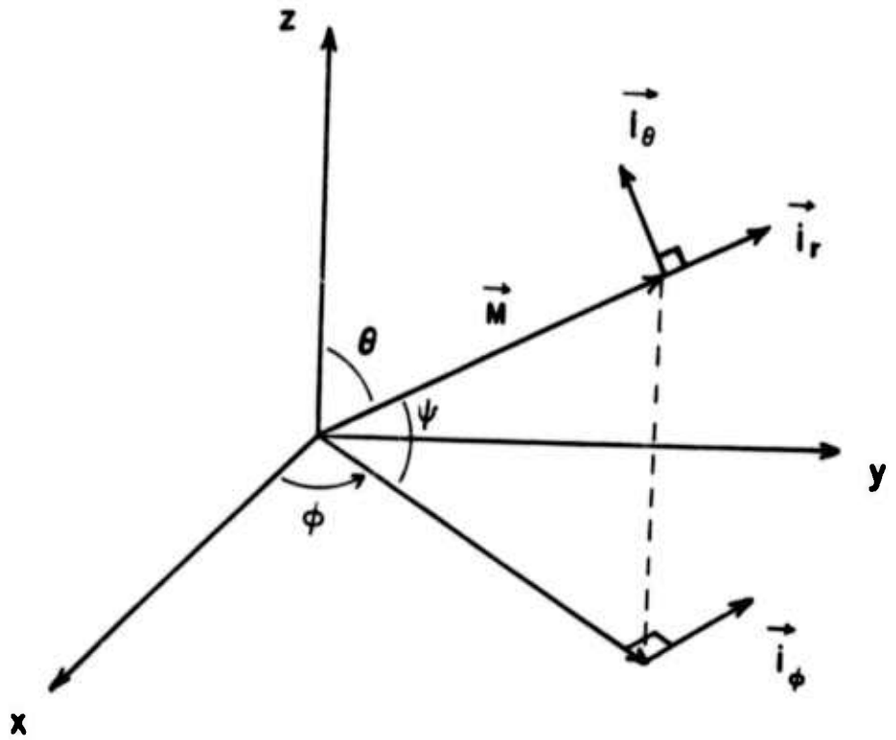

Fig. 3. Magnetization in Spherical coordinates.

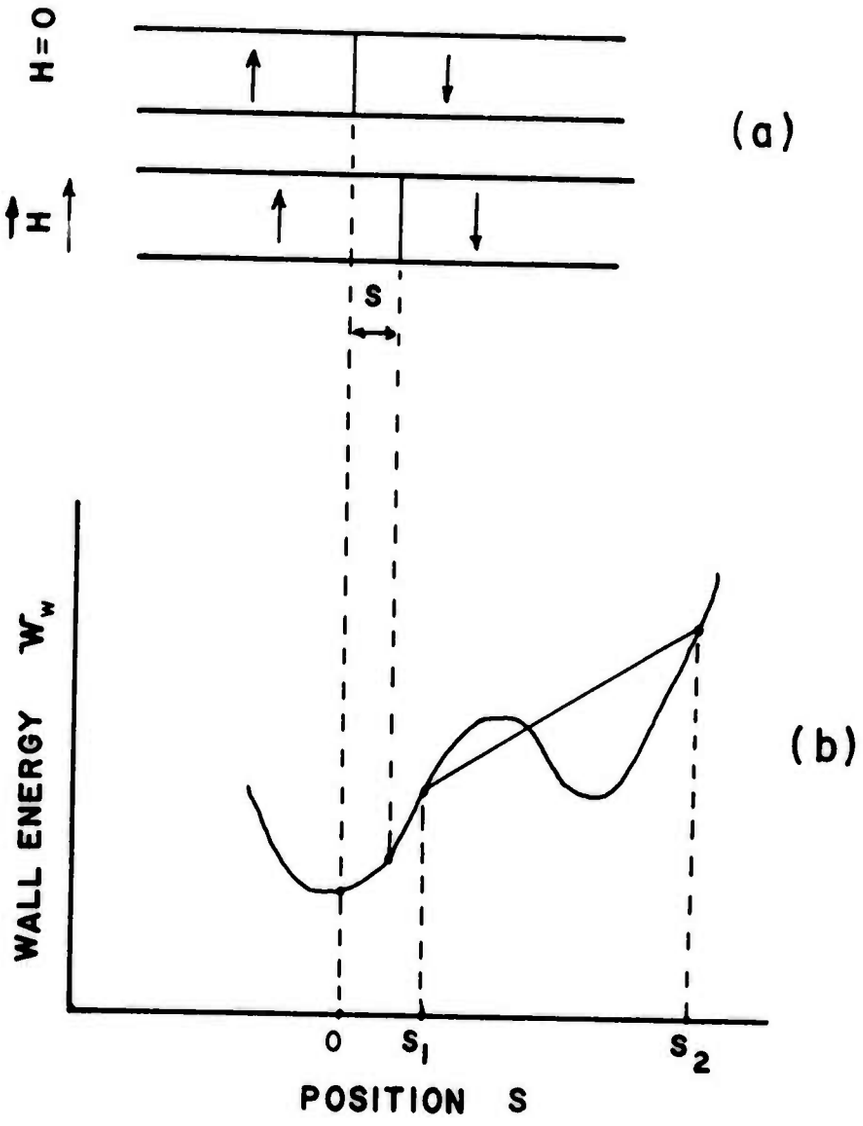

Fig. 4. Domain wall displacement in applied magnetic field.

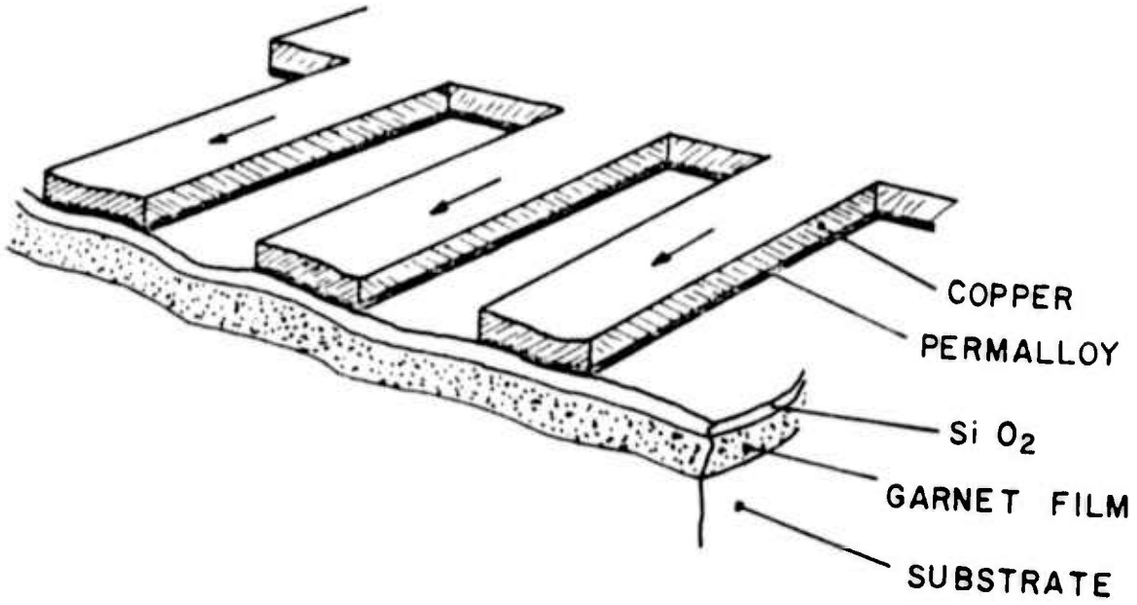

Fig. 5. Configuration of integrated magneto-optical modulator. Current in the copper lines magnetizes the Permalloy which in turn interacts with the Garnet film.

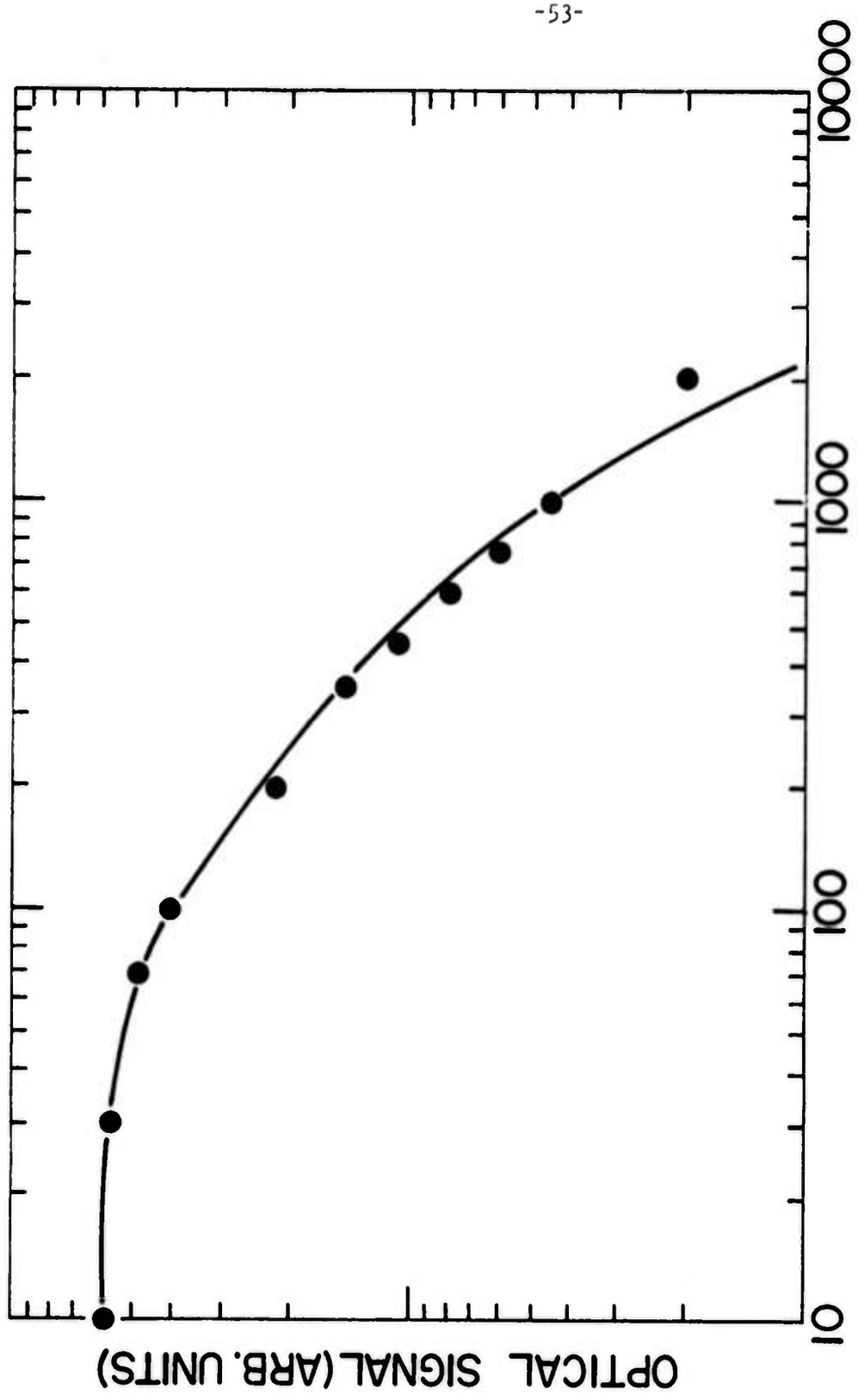

Fig. 6. Frequency response of the device shown in Fig. 5 driven with 400 mA peak to peak.

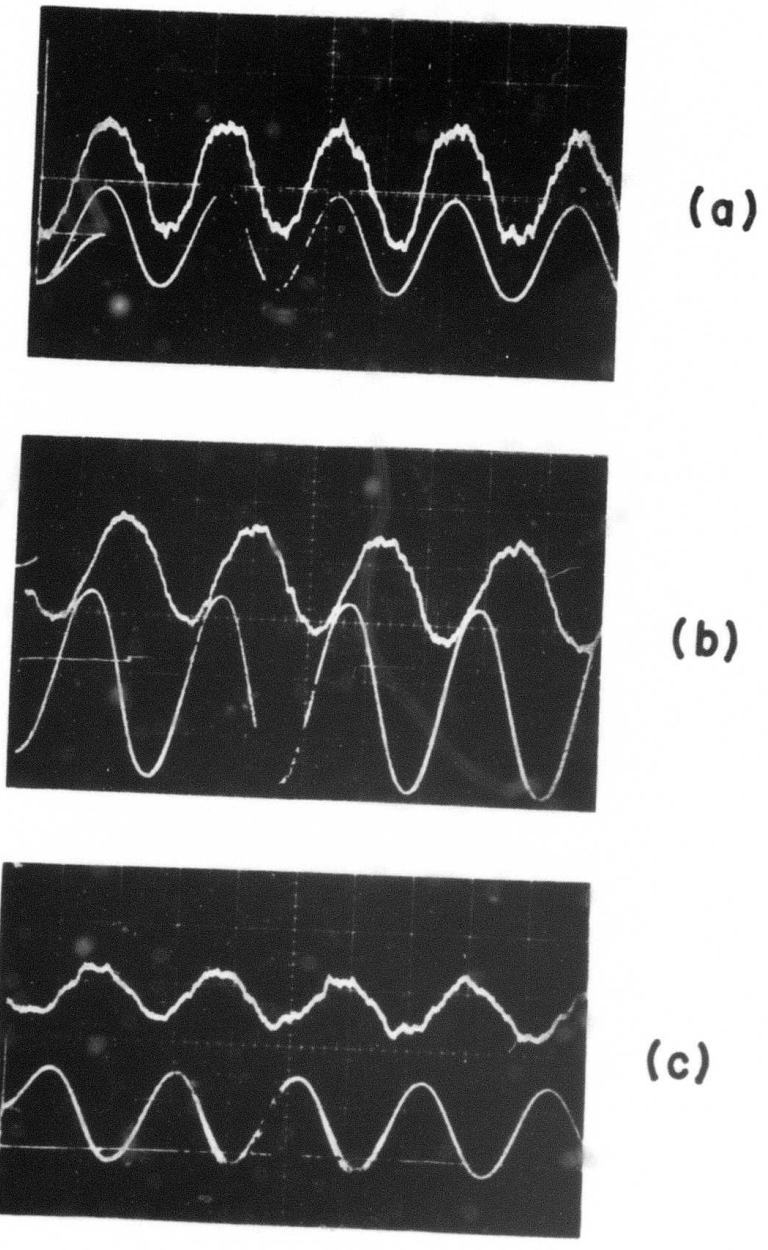

Fig. 7. Illustrating the phase lag between optical signal and driving current for the device shown in Fig. 5. Frequencies are 10 kHz (a), 500 kHz (b) and 1 MHz (c).

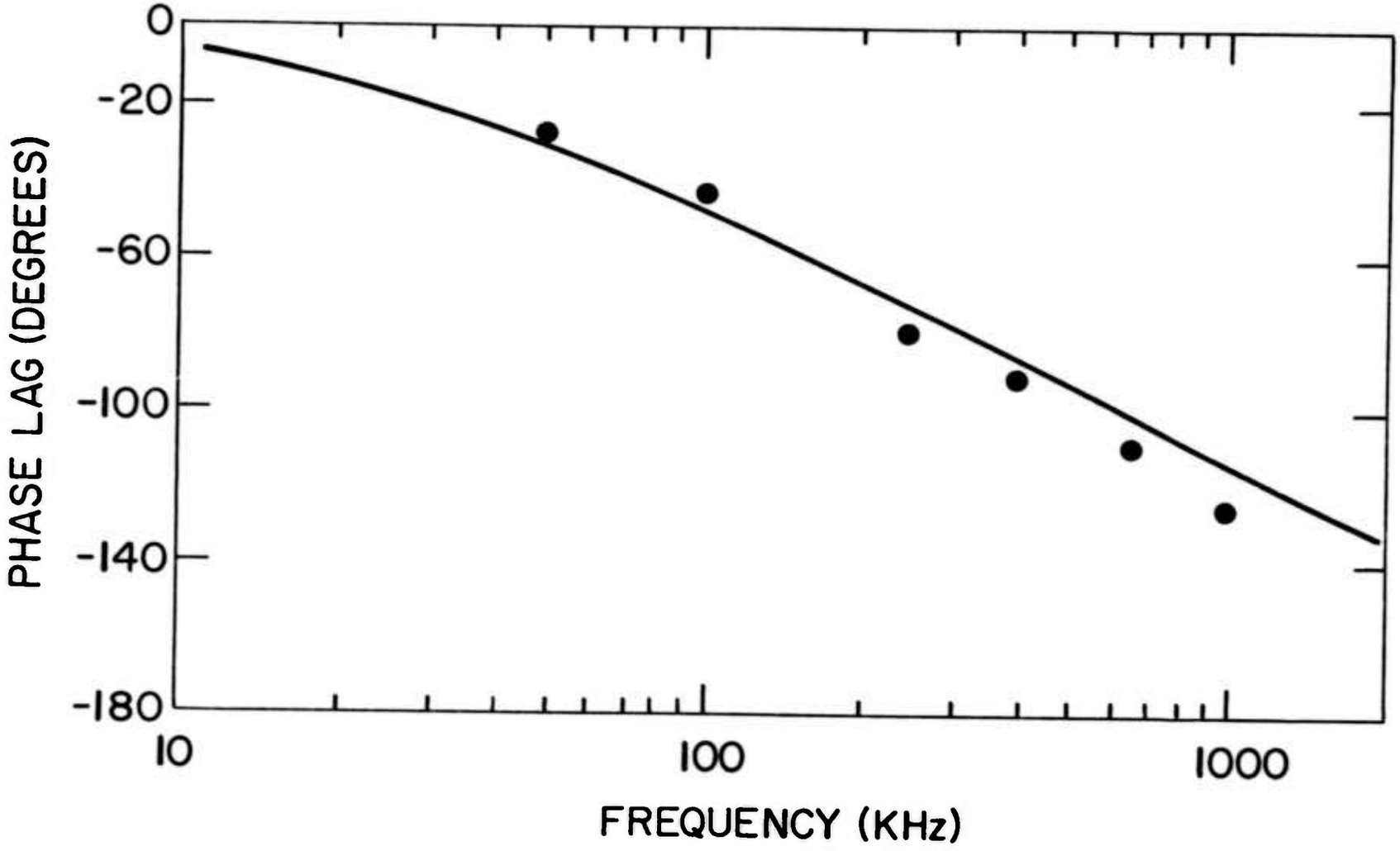

Fig. 8. Phase lag of optical signal relative to driving current vs frequency for device shown in Fig. 5

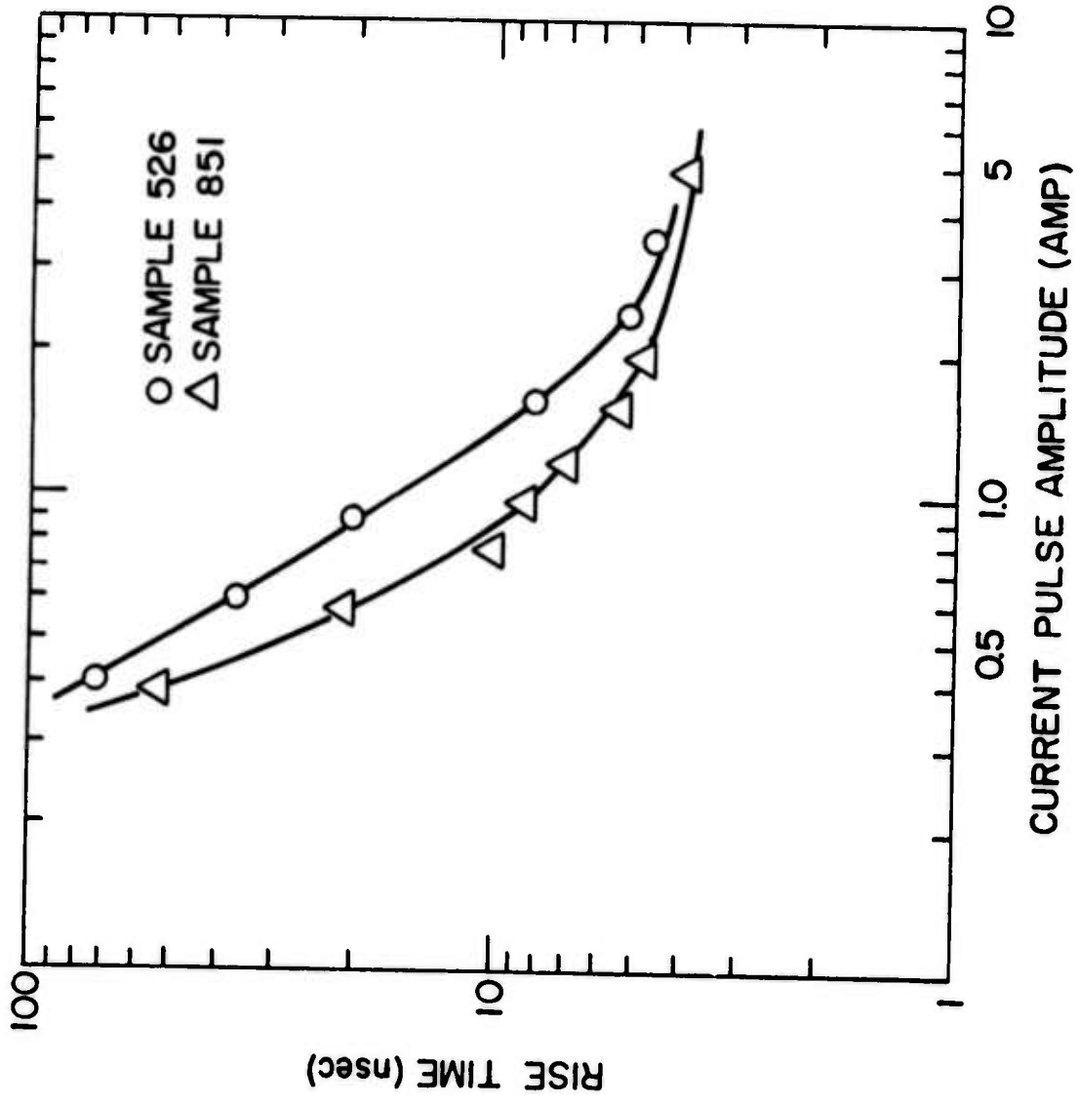

Fig. 9. Rise time of optical signal in two typical samples driven by a current pulse in a meander line.

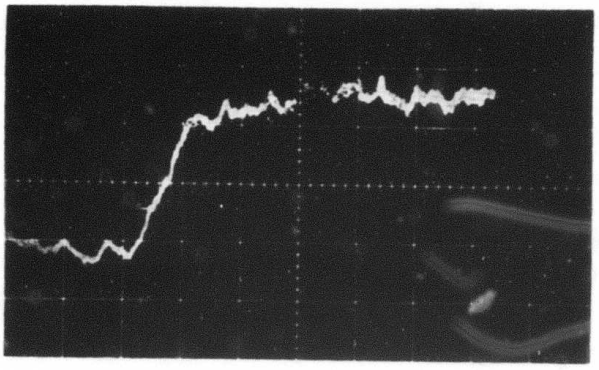

Fig. 10. Optical response in sample #526. Horizontal scale is 5 nsec/cm. Current pulse amplitude was 4 Amps.

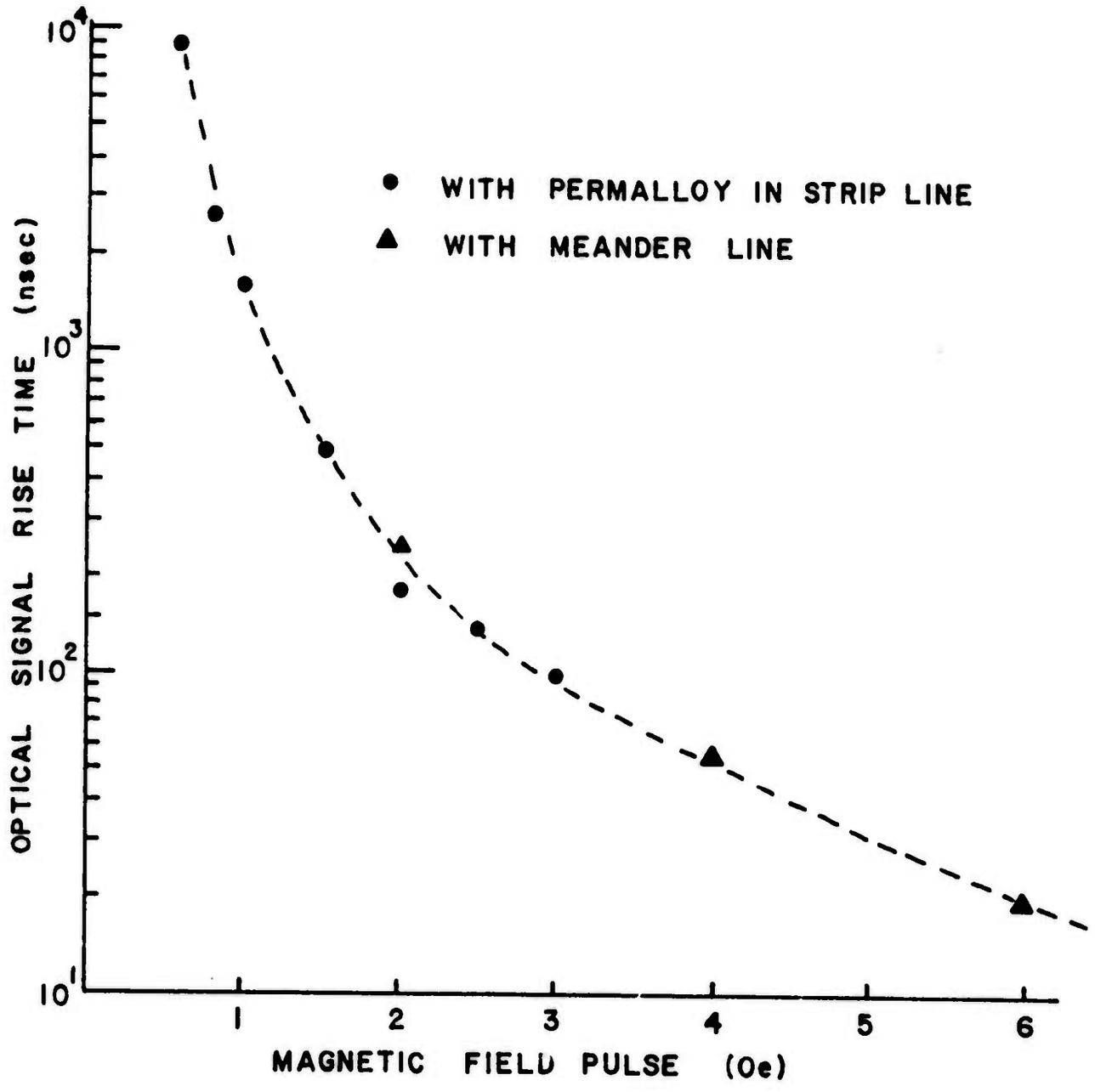

Fig. 11. Optical signal rise time vs amplitude of magnetic field pulses for sample #851 driven either by Permalloy in 50-Ω strip line or by a meander line.

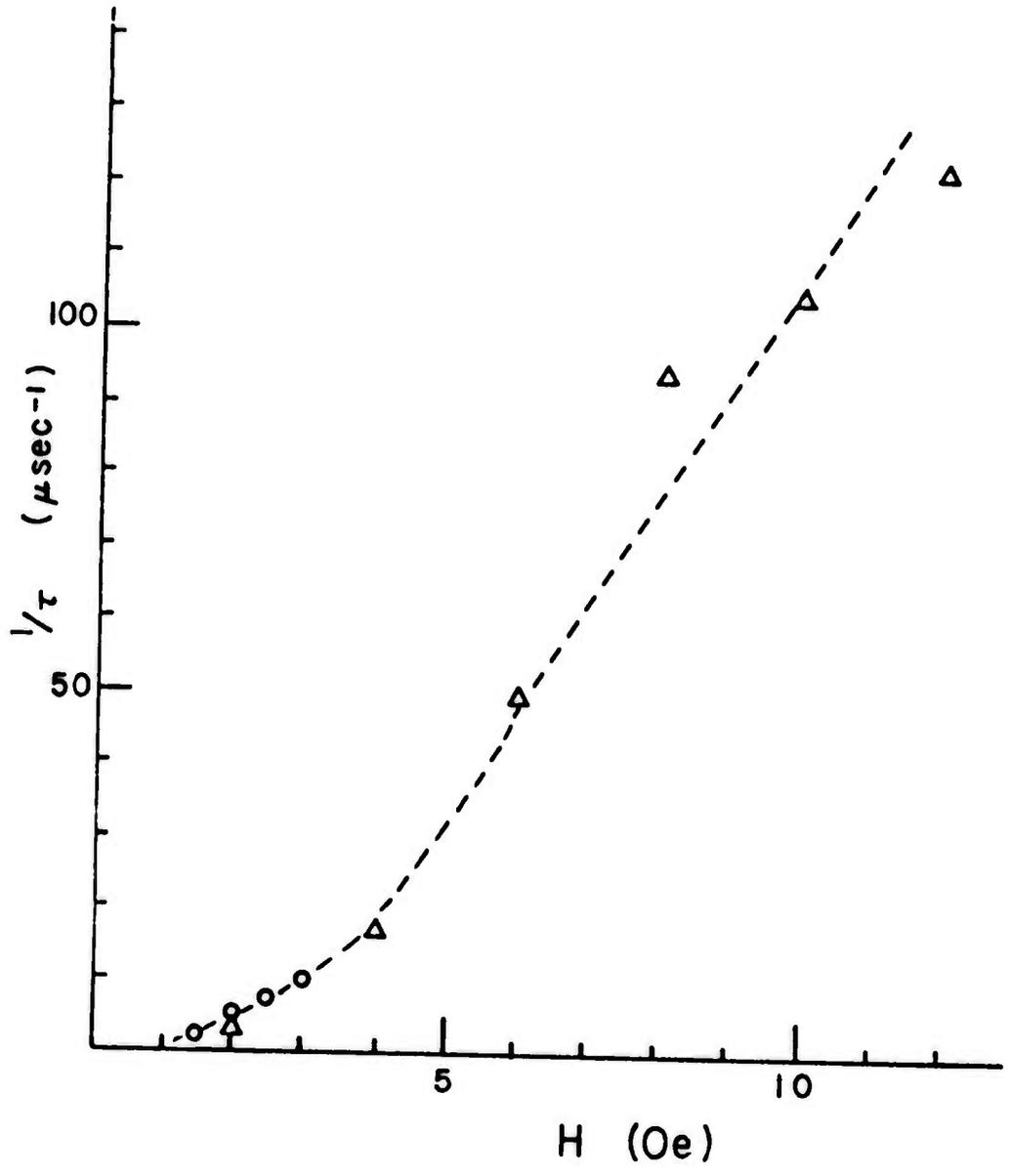

Fig. 12. Inverse switching time in μsec^{-1} vs amplitude of magnetic field pulse.

Figure 5 **Inverse switching time $1/\tau$ vs normalized switching field H_S/H_k for three films of different thicknesses.**
(a) Film 230 B3; 80/20 Ni-Fe; 1100 Å; H_c = 1.8 oe; H_k = 3.0 oe.
(b) Film 215 B2; 80/20 Ni-Fe; 1500 Å; H_c = 1.7 oe; H_k = 3.0 oe.
(c) Film 159 B3; 80/20 Ni-Fe; 2500 Å; H_c = 1.2 oe; H_k = 3.0 oe.

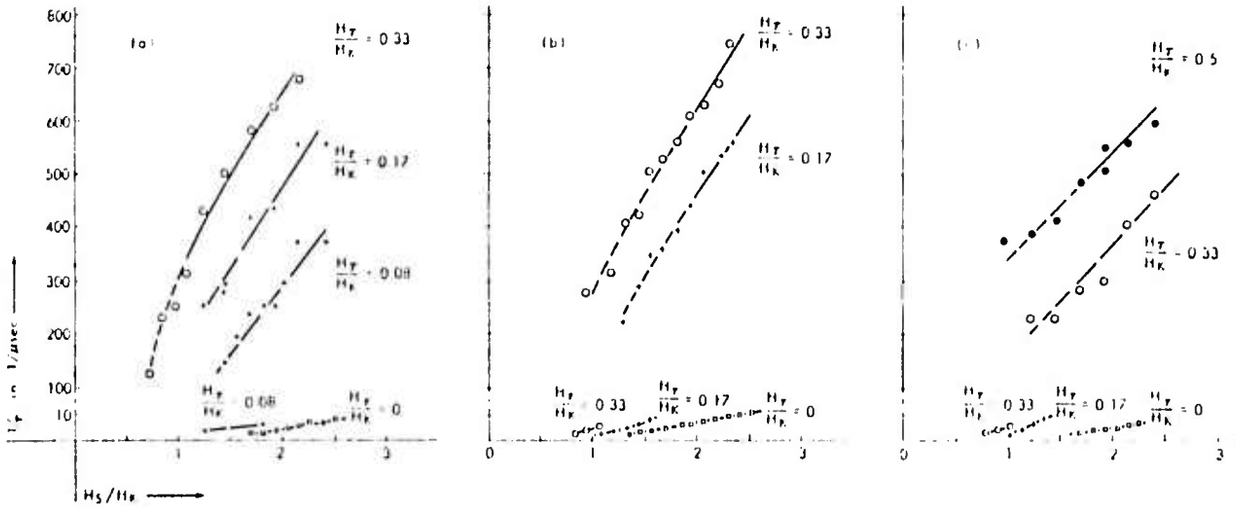

Fig. 13. Results of Dietrich et al, from ref. 23. Notice the trend similar to our Fig. 12.